Carbon – Science and Technology

ISSN 0974 – 0546

http://www.applied-science-innovations.com

ARTICLE Received : 12/7/2013, Accepted : 22/09/2013

Advanced (Non-Carbon) Materials

Preparation, characterization and photocatalytic activity of Fe_2O_3/ZnO and Fe_3O_4/ZnO

Patij Shah(*), K. S. Siddhapara, D. V. Shah

Department of Applied Physics, Sardar Vallabhbhai National Institute of Technology, Surat – 395007, Gujarat, INDIA.

***Corresponding Author**, Tel: +91-0261-2201725/+91-9825191019; Fax:+91-0261-2228394.

Abstract : Composite Iron oxide-Zinc oxide (α-Fe_2O_3/ZnO and Fe_3O_4/ZnO) was synthesized by two-step method. In the first step, uniform α-Fe_2O_3 and Fe_3O_4 particles were prepared through a hydrolysis process of ferric chloride at 80°C. In the second step, the ZnO particles were included in the α-Fe_2O_3 and Fe_3O_4 particles by a zinc acetate [$Zn(Ac)_2 \cdot 2H_2O$] assisted hydrothermal method at low temperature (90 °C). X-ray Powder Diffraction (XRD), Scanning Electron microscopy (SEM), Energy-dispersive X-ray spectroscopy (EDAX) was used to study its structural properties. The α-Fe_2O_3 and ZnO phases were identified by XRD, energy dispersive X-ray analysis (EDAX). The photoactivities of α-Fe_2O_3/ZnO and Fe_3O_4/ZnO nanoparticles under UV irradiation were quantified by the degradation of formaldehyde. The determination of magnetic property was also carried out by Gouy balance method.

Keywords : Photocatalytic activity, two step method, Nano composite.

Introduction : Many conventional methods have been proposed to treat industrial effluents and each method has its shortcomings [1 – 3]. In the last decade advanced oxidation processes (AOPs) have been shown to be effective for the destruction of refractory pollutants. They are based on the generation of highly reactive and oxidizing hydroxyl radicals. O_3/UV, H_2O_2/UV, Fe_2O_3/UV and TiO_2/air/UV are the main types of AOPs that have been suggested [4]. Various combinations of them are employed for the complete mineralization of the pollutants. Reactive oxygen species play a crucial role in heterogeneous photocatalysis aimed at the degradation of organic compounds [5 – 14]. The interest in this area is intense and increasing as shown by the number of publications, which is more than 2000 papers on this topic since 1981 [15]. Several semiconductors (e.g. TiO_2, Fe_2O_3, CdS, ZnS and ZnO) and a couple of semiconductor powders [16, 17] can act as photocatalysts and they have been applied to a variety of problems of environmental interest in relation to water purification.

Formaldehyde is a major pollutant of surface water and ground water, and there are strict limits on the amounts which can be discharged in the effluent. Owing to its stability and solubility in water, the degradation of this compound to a level of safety in the range of 0.1 – 1 mg/l is not easy [1, 18, 19]. The photocatalytic degradation of formaldehyde using TiO_2 has been studied extensively and it is the most promising catalyst due to its high efficiency, stability and low cost [20]. Nevertheless, one disadvantage of TiO_2 for industrial applications is the necessity of filtration after the photo degradation. ZnO has been

reported to be photoactive for formaldehyde degradation in spite of some photocorrosion effects in the liquid–solid phase [21, 22]. α-Fe_2O_3 has also been investigated in the photodegradation of organic compounds under UV radiation, despite the unfavorable position of its oxidative dehydrogenation of n-butane to butenes but its use in photocatalysis has not been reported. In this exploratory work, the synthesis, characterization and preliminary photocatalytic results of Formaldehyde degradation using Fe_2O_3/ZnO and Fe_3O_4/ZnO with UV radiation is reported. These results are compared with the conventional TiO_2.conduction band [23, 24].

Materials and Methods :

Materials : Ferric chloride, $FeCl_3$, HCl, deionized water, $Zn(Ac)_2{\cdot}2H_2O$, Ammonia.

Methods :

1. Preparation and Synthesis :

1.1 Preparation of Fe_2O_3/ZnO and Fe_3O_4/ZnO core/shell particles: Fe_2O_3/ZnO and Fe_3O_4/ZnO core/shell particles were prepared through a hydrolysis process of Zn^{2+} in the presence of Fe_2O_3 or Fe_3O_4 particles. Uniform Fe_2O_3 and Fe_3O_4 particles were also prepared through a hydrolysis process of ferric chloride at 80 °C as literature described. Stock solution of 3M $FeCl_3$ and 0.2 M HCl was mixed in 1:3 ratio, and deionized water was added until final concentration become of Fe^{3+} 0.01 M. This mixture was preserved in water bath at 96 °C for 24 h. Resultant solution was used for further reaction.

Twenty milliliters of Fe_2O_3 or Fe_3O_4 nanoparticles were dispersed in 200 ml deionized. Then 20 mg $Zn(Ac)_2{\cdot}2H_2O$ was introduced to the solution, and the suspension was heated in an water bath at 40 °C under vigorous stirring. Twenty milliliters of 5 % ammonia was added into the suspension in 0.5 hr and the reaction was maintaining the temperature for 1 hour, finally, the colloids were sintered at 550 °C for Fe_2O_3/ZnO and at 350 °C for Fe_3O_4/ZnO for 2 h, yielding the desired nanoparticles in furnace.

2. Physical Characterization :

2.1 X-Ray Diffraction (XRD) Measurement : XRD spectra studies of Fe_2O_3/ZnO nano particles the materials were performed in the Rigaku Miniflex-II Desktop XRD difractometer coupled to a Cu X-ray tube, the Cu-Kα wavelength of which was selected by means of the nickel filter. The crystallite size was calculated from the width of the XRD peaks by using Scherrer formula

$$D = \frac{0.9\lambda}{\beta \cos\theta} \quad (1)$$

where, D is the average crystalline size, λ is the X-ray wavelength used, β is full width at half-maximum intensity and θ is the Bragg's angle in degrees.

2.2 Energy-dispersive X-ray spectroscopy: EDAX of Fe_2O_3/ZnO core/shall nano particles were done by JEOL make Model JSM 5810 LU scanning electron microscope equipped with an X-ray energy dispersive spectroscopy (EDAX)

3. Results and Discussion :

3.1 X-Ray Diffraction (XRD) Measurement : studies of Fe_2O_3/ZnO nano particles the materials were performed in the Rigaku Miniflex-II Desktop XRD difractometer coupled to a Cu X-ray tube, the Cu-Kα wavelength of which was selected by means of the nickel filter.

The chemical composition of the samples was characterized by XRD patterns. Fig. 1 and 2 shows the XRD patterns of Fe_3O_4/ZnO and Fe_2O_3/ZnO, and all the reflection peaks can be readily indexed to a wurtzite phase of ZnO (JCPDS 5-0664) and a hematite phase of Fe_2O_3 (JCPDS 13-0534). The apparent broadening of these peaks indicates fine size of the as-obtained nanoparticles, which is estimated to be about 90 nm from its XRD data. The fact that no distinct peaks existed except the patterns of ZnO and Fe_2O_3 [10, 11].

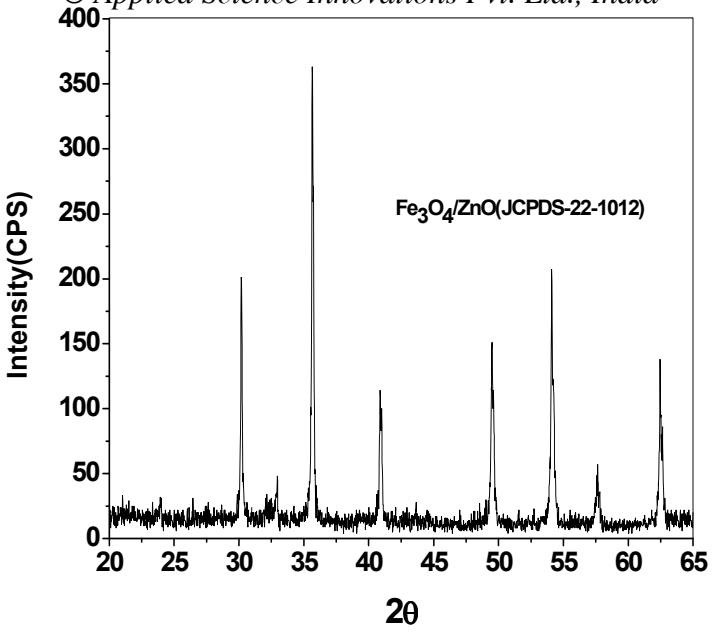

Figure 1: XRD spectra of Fe_3O_4/ZnO Nano particles

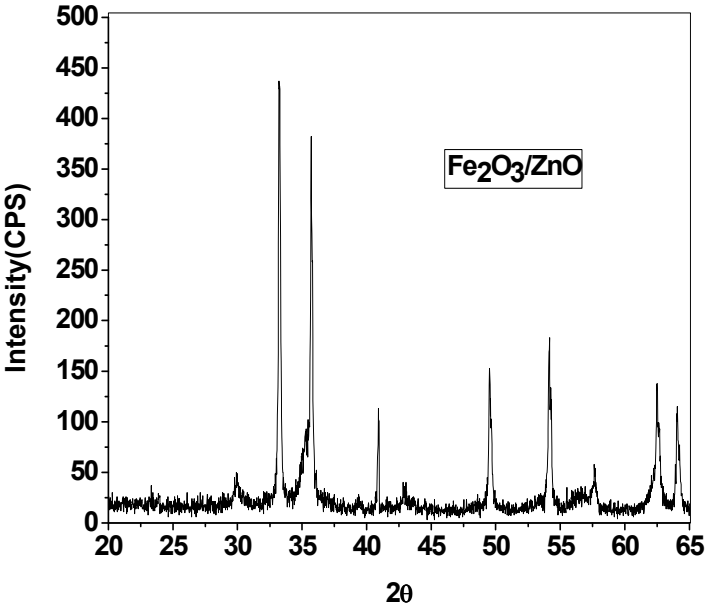

Figure 2: XRD spectra of Fe_2O_3/ZnO Nano particles

3.2.Energy-dispersive X-ray spectroscopy: EDAX of Fe_2O_3/ZnO core/shall nano particles were done by JEOL make Model JSM 5810 LU scanning electron microscope equipped with an X-ray energy dispersive spectroscopy (EDAX). Energy-dispersive X-ray spectroscopy (EDX) shows the elemental signature of presence of O, Fe, and Zn, According to atomic weight stoichiometry corresponding amount of O, Fe, and Zn were observed to be 31.49%, 64.49%, and 1.93% respectively.

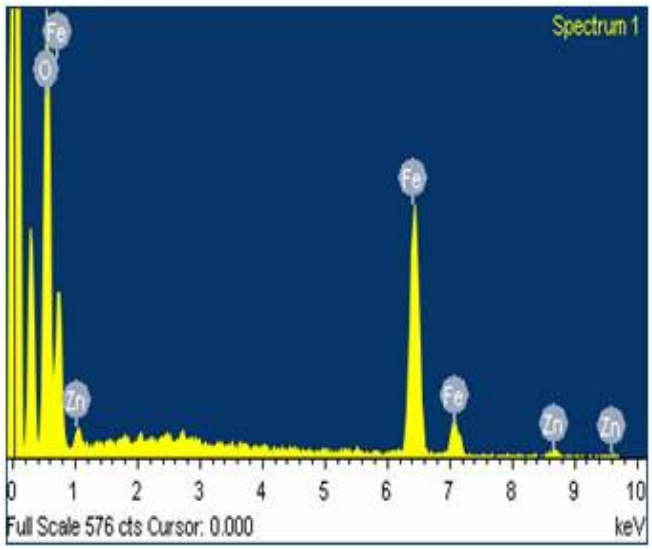

Figure 3 : EDAX Spectra

3.3 UV-Vis Spectroscopy : Absorption spectra were obtained with a Thermo scientific evolution 600 Spectrometer. The samples were placed in a quartz cell for measurement in the range 200-800 nm. The reference used was Ethanol.Figur.4 to 7 shows the absorption spectrum of Fe_2O_3/ZnO, Fe_2O_3, Fe_3O_4 and Fe_3O_4/ZnO nanoparticles suspended in ethanol. Band gaps were calculated from graph using following equation. $E_g=h\upsilon/\lambda$ Where λ is the wavelength, $h\upsilon$ is the photon energy, Calculated band gap E_g from this spectra are mentioned in Table 2 .Due to ZnO coating band gap increases compare to Fe_2O_3, Fe_3O_4, while Fe_3O_4/ZnO shows lower band gap compare to Fe_2O_3/ZnO due to extra oxygen vacancy.

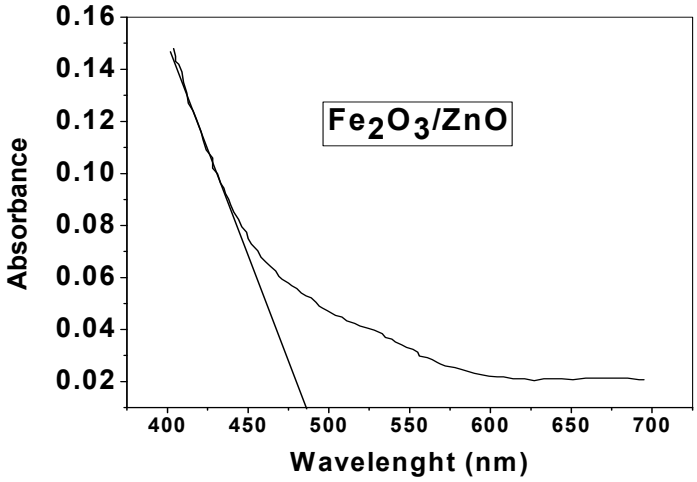

Figure 4: UV-Vis spectra of Fe_2O_3/ZnO Nano particles

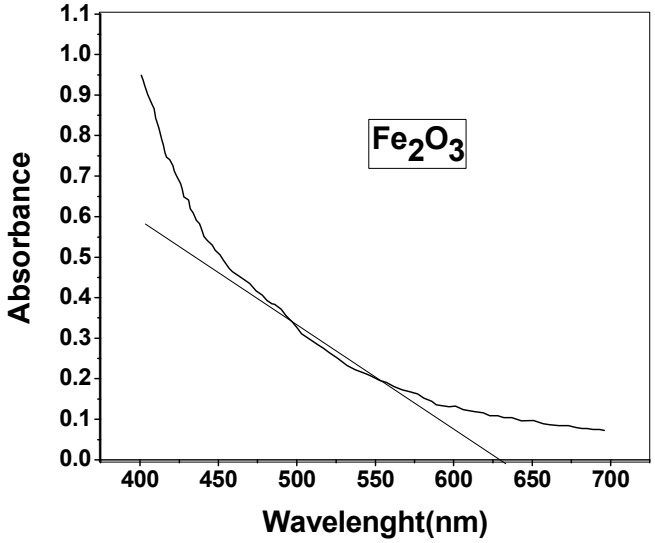

Figure 5: UV-Vis spectra of Fe_2O_3 Nano particles

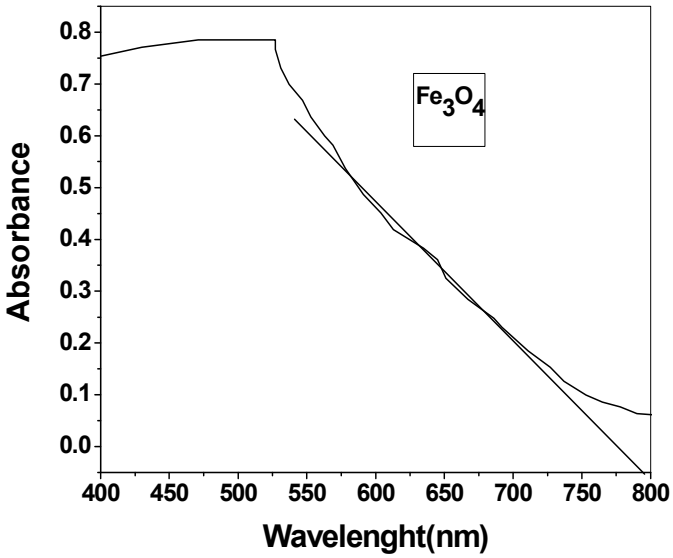

Figure 6: UV-Vis spectra of Fe_3O_4 Nano particles

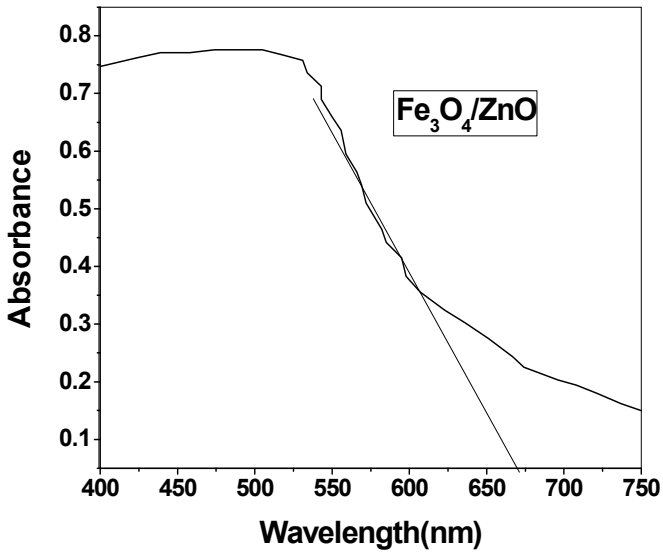

Figure 7: UV-Vis spectra of Fe_3O_4/ZnO Nano particles

3.4 Photocatalytic Behavior :

In Fig. 8, a comparison of photoactivity among TiO_2, ZnO, Fe_2O_3/ZnO and Fe_3O_4/ZnO catalysts at the same operation conditions is shown. Previously, in the absence of illumination or without catalyst, there was no conversion of

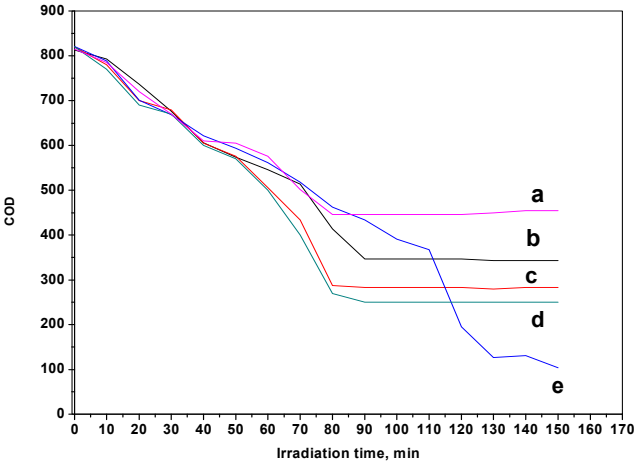

Figure 8: Comparison of Formaldehyde degradation of samples (a) Fe_2O_3 (b) ZnO (c) Fe_2O_3/ZnO (d) Fe_3O_4/ZnO and (e) TiO_2

Formaldehyde. As it is shown in Fig. 5, the conversion of Formaldehyde after 10min of illumination followed the decreased order:

$Fe_3O_4/ZnO > Fe_2O_3/ZnO > TiO_2 \sim ZnO > Fe_2O_3$.

However, after 90min of illumination, the same trend was not followed; with the TiO_2 commercial catalyst, the conversion of formaldehyde was almost twice than that at 1min. The photoactivity of ZnO, Fe_2O_3 and Fe_3O_4/ZnO and Fe_2O_3/ZnO remained constant after 10min of irradiation time,

3.5. Gouy Balance Method:

Magnetic susceptibility has been measured by Gouy balance method. Data obtained from measurement and calculations are as shown in the Table-1, Mass magnetic susceptibility χ_g, Magnetic susceptibility in mole χ_M and Effective magnetic moment μ_{eff} has been calculated by Gouy balance method. χ_g = Magnetic susceptibility was calculated by following equation in grams.

$$\chi_g = [\{\beta\delta + 0.029V\}/m]$$

$$\delta = (A-B) + (F-E)$$

$$m = (E-A)$$

A = Weight of empty tube without field

B = Weight of empty tube with field

β = Balance calibration constant (Calculated in this experiment using a calibration standard.)

E = Weight of tube with sample without field

F = Weight of tube with sample with field

V = Volume

χ_M=Magnetic susceptibility in mole can be calculated by using following formula

$$\chi_M = M\,\chi_g,$$

Where
M = molecular weight of sample

μ_{eff} = Effective magnetic moment has been calculated by following equation

$$\mu_{eff} = 2.828\sqrt{\chi_M T},$$

where T = absolute temperature

βconatant = 772.306 V = 0.303492			A = 16.10265 B = 16.0997		
Sample	**E**	**F**	**m=E-A**	**δ = (A-B) + (F-E)**	**χg**
Fe_2O_3	**16.6583**	**16.69985**	**0.55565**	**0.0445**	**6.1867 E-05**
Fe_2O_3/ ZnO	**16.32295**	**16.3267**	**0.2203**	**0.0067**	**2.35282 E-05**
Fe_3O_4	**16.3108**	**16.3267**	**0.20815**	**0.01885**	**6.99821 E-05**
Fe_3O_4/ ZnO	**16.32184**	**16.3267**	**0.21919**	**0.00781**	**2.75583 E-05**

Table 1: Mass Magnetic Susceptibility of sample mention in table

According to our measurement of the magnetic property, it can be seen that magnetic susceptibility of the Fe_2O_3, Fe_3O_4 is more compare to Fe_2O_3/ZnO, Fe_3O_4/ZnO respectively.

4. Conclusion :

Fe_2O_3/ZnO and Fe_3O_4/ZnO were synthesized by hydrolysis process, and characterized by XRD, UV–Vis, tested in Formaldehyde photodegradation. The results showed a synergism between ZnO and Fe_2O_3, resulting in slightly more active Fe_2O_3/ZnO and Fe_3O_4/ZnO catalyst than ZnO and Fe_2O_3. The photoactivity of ZnO, Fe_2O_3 and Fe_2O_3/ZnO and Fe_3O_4/ZnO remained constant after 10min of irradiation time, which was explained in terms of the large amount of sub products binding to the surface of the catalysts and inhibiting the Formaldehyde adsorption. The decreased order of photoactivity was as follows: TiO_2 > Fe_3O_4/ZnO > Fe_2O_3/ZnO > ZnO > Fe_2O_3. Future work is in progress in order to find the operation conditions of a higher photodegradation of Formaldehyde. The results obtained in this research contribute to the understanding of growth of Fe_2O_3/ZnO and Fe_3O_4/ZnO composite particles, and might lend information to the efforts of enhancing their environmental application.

References :

[1] D.H.F. Liu, B.G. Liptak (Eds.), Environmetal Engineers Handbook, Chapman and Hall/CRC Press, Cnet Base, 1999.

[2] S. Hamoudi, F. Larachi, A. Sayari, J. Catal. 177 (1998) 247.

[3] F. Luck, Catal. Today. 53 (1999) 81.

[4] R. Andreozzi, V. Caprio, A. Insola, R. Marotta, Catal. Today. 53(1999) 51.

[5] L. Davydov, P.G. Smirniotis, J. Catal. 191(2000)105.

[6] J. Peral, X. Domechech, D.F. Ollis, J. Chem. Biotechnol. 70 (1997)117.

[7] A. Fujishima, T.N. Rao, D.A. Tryc, J. Photochem. Photobiol. C 1(2000) 1.

[8] N. Serpone, A. Salinaro, A. Emeline, V. Ryabchuk, J. Photochem. Photobiol. A 130 (2000) 83.

[9] J.M. Herrmann, Catal. Today 53 (1999) 115.

[10] C.S. Turchi, D.F. Ollis, J. Catal. 122 (1990) 178.

[11] E. Pelizzetti, C. Minero, Electrochim. Acta 38 (1993) 47.

[12] A.L. Linsebigler, G. Lu, J.T. Yates, Chem. Rev. 95 (1995) 735.
[13] M.R. Hoffmann, S.T. Martin, W. Choi, D.W. Bahnemann, Chem. Rev. 95 (1995) 69.
[14] A. Mills, S. Le Hunte, J. Photochem. Photobiol. A 108 (1997) 1.
[15] D.F. Ollis, C.R. Acad. Sci. Paris, Série Iic, Chimie/Chemistry. 3(2000) 405.
[16] A. Di Paola, L. Palmisano, A.M. Venezia, V. Augugliaro, J. Phys.Chem. B 103 (1999) 8236
[17] A.M. Peiró, J.A. Ayllón, J. Peral, X. Doménech, Appl. Catal. B 30 (2001) 359
[18] A.A. Yawalkar, D.S. Bhtkhande, V.G. Pangarkar, A.A.C.M. Beenackers, J. Chem. Technol. Biotechnol. 76 (2001) 363.
[19] D.F. Ollis, E. Pelizzetti, N. Serpone, Environ. Sci. Technol. 25 (1991) 1523.
[20] G. Marc´ ı, V. Augugliaro, M.J. López-Muñoz, C. Mart´ ın, L. Palmisano, V. Rives, M. Schiavello, R.J.D. Tilley, A.M. Venezia, J. Phys. Chem. B. 105 (2001) 1033.
[21] J. Villaseñor, P. Reyes, G. Pecchi, J. Chem. Technol. Biotechnol. 72 (1998) 105.
[22] B. Pal, M. Sharon, J. Chem. Technol. Biotechnol. 73 (1998) 269.
[23] H. Armendariz, G. Aguilar, P. Salas, M.A. Valenzuela, I. Schifter, H. Arriola, N. Nava, Appl. Catal. A. 92 (1992) 29.
[24] Z. Ding, G.Q. Lu, P.F. Greenfield, J. Phys. Chem. B. 1